Structural testing and numerical modelling of a glass fibre-reinforced composite demonstrator for tidal turbine blades

Yadong Jiang, William Finnegan, Conor Kelly, Ahmed Bastawisy, Tomas Flanagan, Conor Glennon, and Jamie Goggins

Abstract—**Tidal energy, a clean, predictable and reliable renewable energy source, can play an important role in creating a carbon-free energy system in Europe. The cumulative tidal stream technology deployed in Europe was 30.2 MW in 2022, which contributes to 77% of the global total tidal energy device installations. Under a high growth scenario, approximately 2388 MW of tidal energy capacities will be deployed in Europe by 2030. The structural performance of a tidal turbine blade is vital as it guarantees the safe operation of a turbine within its lifespan in marine environments. Experimental testing is a reliable way of investigating the structural performance of a tidal turbine blade. In this research, the structural performance of a composite demonstrator is carried out. The 5 m long demonstrator represents a tidal current turbine's main structure, the strongest region of a typical rotor blade. The demonstrator consists of two spar cap and two webs, which are manufactured with glass-fibre reinforced composite materials. Steel inserts are drilled into the root of the spar cap to connect to the support frame. A hydraulic actuator is used to apply loading to the tip region of the demonstrator to simulate the operation loading. Instrumentations, including strain gauges, accelerometers and displacement transducers, are installed to monitor the demonstrator responses. The test results are utilised to validate a finite element model, which will be used in the blade design and optimisation case study in the future.**

Keywords— **Composite Materials, Experimental Testing, Finite-Element Model, Renewable Energy, Structural Performance, Tidal Energy, Tidal Turbine.**

Sponsor and financial support acknowledgement: This work was funded by the Sustainable Energy Authority of Ireland (SEAI) under the SEAI Research, Development, and Demonstration Funding Programme 2021 (grant numbers21/RDD/630, 21/RDD/655 and 21/RDD/601). The research was also supported by Science Foundation Ireland (SFI) through the MaREI Research Centre for Energy, Climate, and Marine (grant no 12/RC/2302_2). The authors would also like to acknowledge the support of Marine Institute, funded under the Marine Research Programme by the Government of Ireland (PDOC/21/03/01).

Y. Jiang is with the SFI MaREI Centre, Ryan Institute, School of Engineering, University of Galway, University Road, Galway, H91 TK33 Ireland. (e-mail: yadong.jiang@universityofgalway.ie).

W. Finnegan is with Construct Innovate and the SFI MaREI Centre, Ryan Institute, School of Engineering, University of Galway, University Road, Galway, H91 TK33 Ireland. (e-mail: william.finnegan@ universityofgalway.ie).

C. Kelly is with ÉireComposites Teo, Galway, H91 Y923 Ireland. (e-mail: c.kelly@eirecomposites.com).

A. Bastawisy is with ÉireComposites Teo, Galway, H91 Y923 Ireland. (e-mail: a.bastawisy@eirecomposites.com).

T. Flanagan is with ÉireComposites Teo, Galway, H91 Y923 Ireland. (e-mail: t.flanagan@eirecomposites.com).

C. Glennon is with the SFI MaREI Centre, Ryan Institute, School of Engineering, University of Galway, University Road, Galway, H91 TK33 Ireland. (e-mail: conor.glennon@universityofgalway.ie).

J. Goggins is with Construct Innovate and the SFI MaREI Centre, Ryan Institute, School of Engineering, University of Galway, University Road, Galway, H91 TK33 Ireland. (e-mail: conor.glennon@universityofgalway.ie).

Digital Object Identifier: https://doi.org/10.36688/ewtec-2023-181

I. INTRODUCTION

Renewable energy plays a key role in achieving net-zero carbon emission targets as it produces no greenhouse gas emissions and eases air pollution. Tidal energy is a predictable and reliable renewable energy. Tidal movements are reliably constant since the moon's phases are very predictable. This makes tidal energy more predictable than many other renewable energy sources such as wind and solar power. Tidal turbines convert tidal energy to electricity. Compared to wind turbines, it does not produce a lot of noise and vibration. In 2021, there are 2.2 MW of tidal energy devices deployed in Europe, making the total capacity boosted to 30.2 MW since 2010 (OEE [1]).

The structural performance of the rotor blade, an important part of the tidal turbine, is vital to ensure the safe operation of the turbine. Performing physical testing is an efficient way to investigate the blade's structural performance, where the state-of-the-art review is available in Munaweera Thanthirige et al. [2]. Glennon et al. [3] carried out experimental testing on two tidal turbine blades, designed for a 70 kW tidal energy device. The structural strength and design life of the blades were verified through static and accelerated-life testing, respectively. A full-scale tidal turbine blade was manufactured and tested by Finnegan et al. [4]. This 8 m blade is manufactured for a 1 MW tidal turbine, one of the world's largest tidal energy devices. Through dynamic, static and fatigue testing, the blade was proved to have a service life of over 20 years and can survive under extreme operating conditions. Besides physical testing, numerical analysis is widely used in studying the structural performance of tidal turbine blades. Similar to wind turbine blades, shell elements were commonly used to build the finite element model of a tidal turbine blade. Fagan et al. [5] utilised finite element analysis to design the structures of a tidal turbine blade. Based on the stress given by the shell elements, a blade with good structural responses was designed. The finite element model of an 8 m tidal turbine blade, made using glass fibre-reinforced composite material, was proposed by Jiang et al. [6]. By validating against physical testing data, good accuracy of the developed model was demonstrated.

However, there is still a scarcity of literature on structural performance investigations of tidal turbine blades. In the paper, a demonstrator which represents the main structure of a tidal turbine blade is manufactured and its structural performance is investigated. Through physical testing and numerical analysing, the demonstrator's responses under flexural loading are examined.

II. Materials and Methodology

A. *Aim, Objectives and Methodology*

The main aim of this study is to investigate the structural performance of a 5 m composite blade demonstrator. To achieve this aim, the following objectives will be accomplished:

1) Manufacturing a 5 m composite blade demonstrator, using glass fibre-reinforced composite materials, to represent the main structure of a tidal turbine blade.
2) Performing full-scale experiment tests to verify the structural performance of the demonstrator.
3) Developing and validating the finite element model using the testing results.

The study of the demonstrator structural performance contains three stages, namely the manufacture, testing and numerical analysing. This 5 m composite structure was manufactured by ÉireComposites using resin-infusion technology. The demonstrator then underwent a series of load cases to explore its stiffness and strength, in line with the IEC testing standard. A comprehensive finite element model was developed to predict the structural responses of the demonstrator.

B. *Composite demonstrator*

In general, wind turbines and tidal turbines use similar principle to convert kinematic energy to mechanical energy. Hence, tidal turbine blades and wind turbine blades share the same structure design methodology. However, since the water density is about 840 times larger than that of air, tidal turbines are smaller than wind turbines with the same power production capacity. This also means that the tidal turbine blades suffer much higher loads compared to that of wind turbine blades with the same length. Similar to modern wind turbine blades, tidal turbine blades are mainly manufactured using carbon fibre-reinforced [4] or glass fibre-reinforced composite materials [3]. Tidal turbine blades are generally stronger and heavier than wind turbine blades due to higher service loads. Fig. 1 shows the shape of a typical tidal turbine blade. The centre region of the external shell is strengthened with extra composite materials. This allows the blade to resist the flexural force effectively. Together with the webs inside the blade, it forms the main structural part of the blade. This part plays an important role in the structural performance of the tidal turbine blade. Hence, it is necessary to study the structural performance of this main structure under flexural loading.

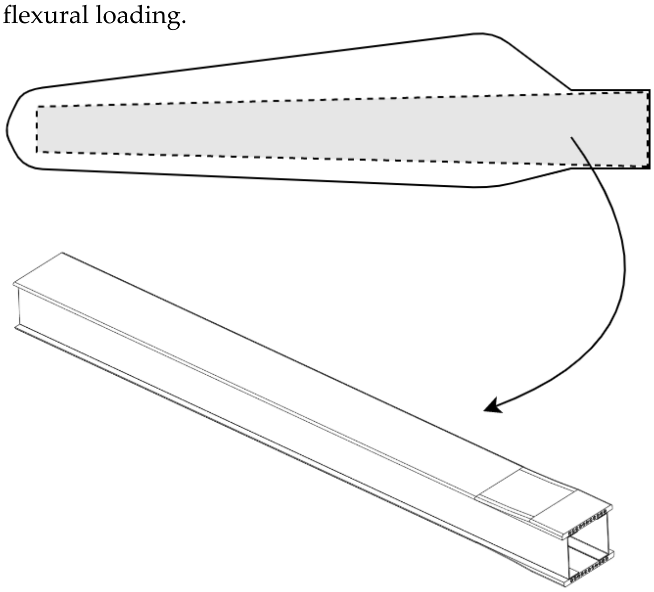

Fig. 1. Simplification of the main structure of a tidal turbine blade.

In this research, a 5 m composite blade demonstrator was manufactured to represent the structural part of a tidal turbine blade, as shown in Fig. 1. It was made with glass fibre-reinforced composite material and underwent a series of experimental tests. The main structural part of the tidal turbine blade was simplified to a rectangular demonstrator. Conducting experiments on the demonstrator can de-risk the tidal turbine blade by ensuring it can withstand the maximum loads. Moreover, the testing data can validate the developed numerical model, which can be used in the design of the next-generation tidal turbine blade.

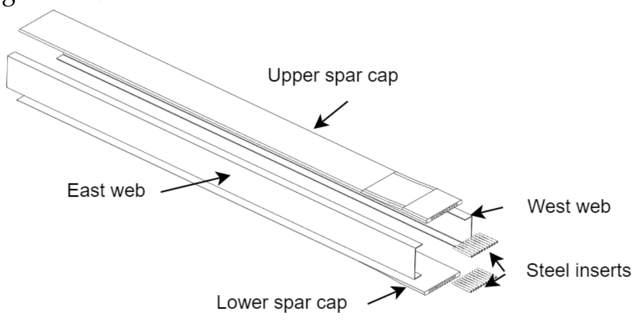

Fig. 2. Structure details of the demonstrator.

Structural details of the demonstrator are shown in Fig. 2. The two spar caps were manufactured using unidirectional glass fibre-reinforced composite materials (UD). The spar cap has a thickness of 15 mm since it is the main component to resist flexural loading. The thickness of the spar cap root was increased to 40 mm as the root of the demonstrator was embedded with 11 steel inserts. These steel inserts are used to connect the demonstrator to a support structure through M10 bolts. With the root thickness increased and steel inserts embedded, the root of the demonstrator is the strongest region. This helps the demonstrator to resist the flexural loading since the root subjects to the highest bending moment. The two webs have a channel shape cross-section and a uniform thickness of 6 mm. They were made from tri-axial glass fibre-reinforced composite materials (TX). Both spar cap and web are manufactured using epoxy resin infusion techniques. Fig. 3 shows the manufactured demonstrator. Each component of the demonstrator was manufactured individually and assembled using adhesive.

Fig. 3. The demonstrator manufactured by ÉireComposites Teo, Galway, Ireland

C. *Experimental testing*

Physical tests are conducted to examine the structural performance of the demonstrator. Tests were carried out in the Large Structures Testing Laboratory of the University of Galway. The natural frequencies, stiffness and strength of the demonstrator are of interest. The obtained test results are used to develop a finite element model, which can contribute to the design of full-scale tidal turbine blades. The testing program contains natural frequency (dynamic) tests and static tests, which are conducted under the instructions given by testing standard IEC 61400–23 [7]. As shown in Fig. 4, the demonstrator is fixed at the root using two steel structures, namely the steel adaptor and support frame. 22 M10 bolts and 30 M40 bolts are employed to constrain the demonstrator and steel adaptor, respectively. The support frame is directly mounted to the strong reinforced-concrete reaction floor of the laboratory.

In the natural frequency tests, the demonstrator is vibrated in the horizontal and vertical directions, by applying a transient impact to its tip. There are 3 accelerometers and 1 accelerometer installed on the upper spar cap and the east web, respectively, to record the blade vibration. Fast fourier transform (FFT) techniques are utilised to analyse the natural frequencies based on the recorded acceleration.

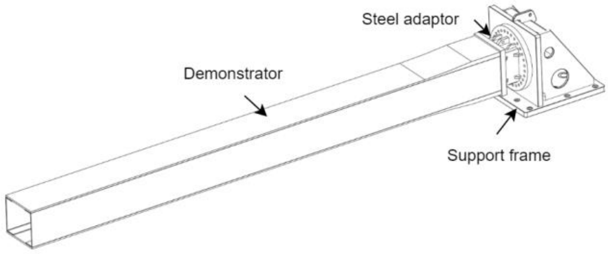

Fig. 4. Fixing mechanism of the demonstrator for testing

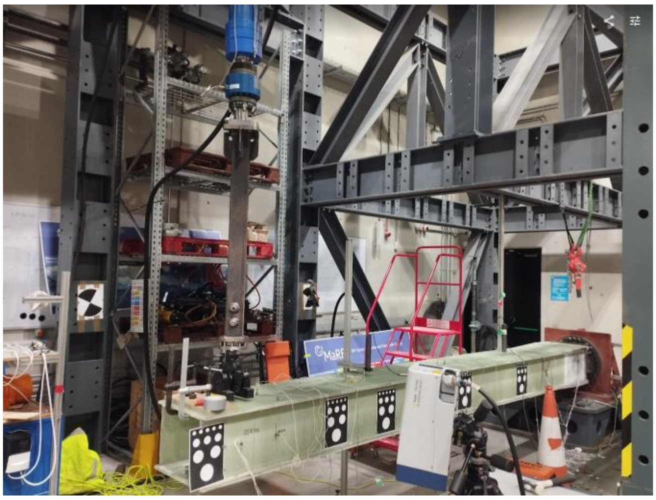

Fig. 5. Test setup in the Large Structures Laboratory of University of Galway

During the static tests, the composite blade demonstrator is loaded at the tip region using a 250 kN hydraulic actuator. As shown in Fig. 5, this vertical load introduces a linear moment diaphragm along the demonstrator length. The force is applied in the downward direction and a steel plate is placed under the actuator to distribute the load to the spar cap surface. There are four load cases considered in the test programme, with maximum loads applied listed in Table I. Besides the forces and displacements provided by the actuator, strain gauges and displacement transducers are installed to monitor the responses of the demonstrator. For each spar cap, there are five linear strain gauges installed along the component to inspect the fibre direction strain development. Three displacement transducers, including one string potentiometer (at tip) and two Linear Variable Differential Transformers (LVDTs), are installed along the lower spar cap to record the demonstrator deflections. Apart from the instruments on the demonstrator, the responses of the steel adaptor, which is used to constrain the demonstrator, are also monitored. Two linear strains are fitted on the upper and lower surface of the steel adaptor, aiming to ensure that the steel fixture does not yield before breaking the demonstrator. It should be noted that the steel fixtures may develop movements under the testing load due to its flexibility. Hence, two LVDTs are installed on the front surface of the adapter. The measured displacements can be used to calculate the rotation of the steel fixtures. This rotation can result in an overestimation of the demonstrator deflection and should be eliminated in the data post-processing.

TABLE I
MAXIMUM LOAD APPLIED IN EACH LOAD CASE

Load case #	Maximum force [kN]
1	9.4
2	19.4
3	24.0
4	30.1

D. Numerical model

A finite element model is developed to predict the structural response of the demonstrator. The model is created in the finite element software Ansys [8], as shown in Fig. 6. Considering the root thickness of the spar, 40 mm, is relatively thick compared to its width. Solid elements are used to generate the spar cap. Another advantage of using solid elements is that it enables embedding the steel inserts in the root region. As annotated in Fig. 7, the steel inserts and M10 bolts are modelled using solid elements. Modelling the steel inserts, bolts and spar cap as solid elements can increase the accuracy of the finite element model as the stress distribution between the steel inserts and composite spar cap is considered. Different from the spar caps, the webs can be considered to be thin-wall components since their thickness, 6 mm, is relatively small compared to the cross-section size. Hence, the webs are modelled as layered shell elements. The webs and spar caps were assembled using adhesive, which is also considered in the finite element model. As shown in Fig. 7, a layer of solid elements, with a thickness of 1 mm, is generated between the spar cap and the web.

It should be highlighted that in the static tests, both the demonstrator and boundary conditions are symmetric. Taking this advantage, only half of the demonstrator model (Fig. 8) is created in the static analyses, which reduces the complexity of the element number and reduces the analysing time. However, for the modal analysis, the full-scale model is used to capture the modal shape in the horizontal direction (Fig. 6). To simulate the load introduction mechanism, the multipoint constraint elements are employed in the loaded surface.

Fig. 6. Finite element model generated for the natural frequency analysis

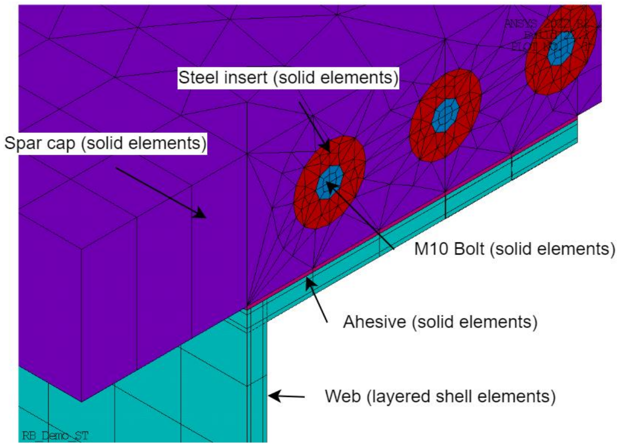

Fig. 7. Details of the finite element model (root region)

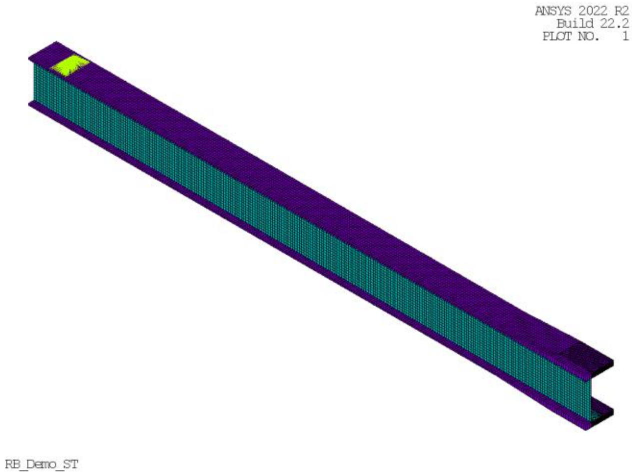

Fig. 8. Finite element model generated for the static analysis

III. RESULTS AND DISCUSSION

E. Experimental results

The first vertical and horizontal natural frequencies of the demonstrator, 13.24 Hz and 12.55 Hz, are obtained from the dynamic tests, with results listed in Table II. Regarding static testing, the demonstrator developed tip deflections of 16.8 mm and 31.7 mm in the first two load cases, respectively. No visual damage was observed in the two load cases. Based on the recording from the strain gauges, all components, both the demonstrator and the steel fixture, were deformed elastically. However, according to the recordings from the two LVDTs installed on the adaptor, there are rotations developed at the demonstrator root, with values of 0.08° and 0.15°, respectively. These rotation values make the demonstrator deflections overestimated. Fig. 9 shows the demonstrator deflection with values corrected based on the obtained root rotations. In the third load case, significant noises were heard under a load of 24 kN. It was observed that part of the adhesive between the upper spar caps and webs cracked. Consequently, the stiffness of the demonstrator dropped significantly. Since the demonstrator was not completely damaged in the third load case. In the fourth load case, the demonstrator was loaded to failure. Under a load of 30.1 kN, some of the steel inserts in the upper spar cap were pulled out (Fig. 10). The demonstrator completely lost its strength. In all load cases, the strain gauges indicated that there were no damages in the composite parts, as shown in Fig. 11.

TABLE II
TEST RESULTS AND NUMERICAL PREDICTION ON NATURAL FREQUENCIES OF THE DEMONSTRATOR (UNIT: HZ)

	Experimental	Numerical	Difference
1st Flapwise	13.24	17.99	36%
1st Edgewise	12.55	16.36	30%

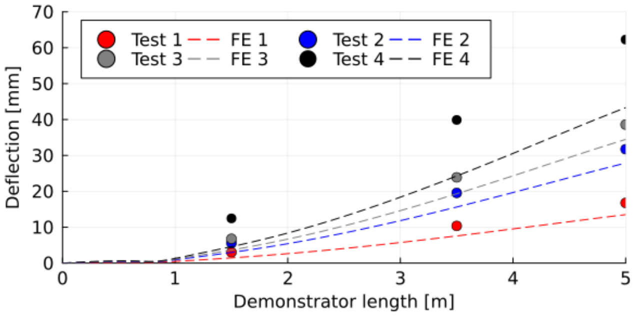

Fig. 9. Deflection of the demonstrator under the four load cases (root rotation corrected)

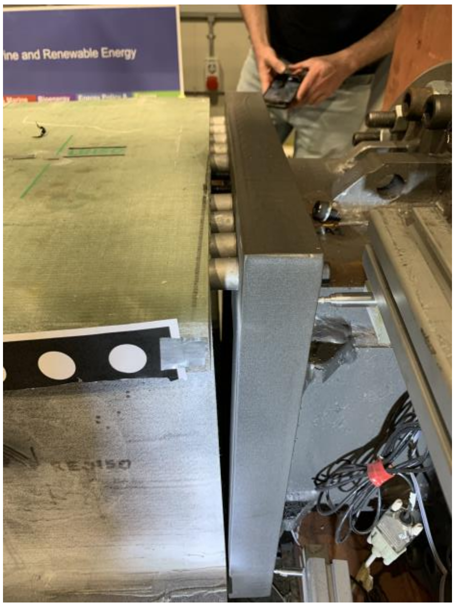

Fig. 10. Steel insert failure at the demonstrator

F. Numerical model validation

To validate the accuracy of the proposed numerical model, the modal analysis and static analyses were carried out. Table II compares the predicted natural frequency values with the test results. The finite element model overestimates the two natural frequencies. This means that the numerical model has higher stiffness than that of the demonstrator. The predicted first vertical and horizontal natural frequencies are 36 % and 30% higher than the test results, respectively. This is caused by the flexibility introduced by the fixtures. The root rotation reduces the obtained natural frequency values. This is in line with the observation from Jiang et al. [6].

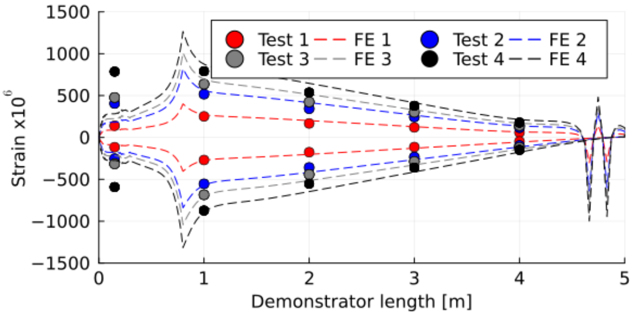

Fig. 11. Strain values on the upper and lower spar caps of the demonstrator

For the static analyses, Fig. 9 and Fig. 11 compare the deflections and strain values between the experimental data and numerical results, respectively. For the first three load cases, the numerical mode predicts reasonably accurate deflections, with an average difference of 14%. It should be noted that the adhesive damage, observed in load case 3, was not captured by the numerical model. Hence, the deflection predicted in load case 4 is less than that from the tests. Regarding the strain prediction, the strain values recorded by the gauges agree well with the numerical results, except for the root strains. The strain values around the root region are generally overestimated. This may be influenced by the flexibility of the steel fixture. As observed in the tests, the steel fixtures deformed together with the root region, and hence, the strain values were overestimated. By applying the failure check based on the maximum stress method, all the composite and steel components do not fail, which is in line with the test observation. Overall, it can be concluded that the developed finite element model has good accuracy. But it cannot capture the failure of the interface failure between the steel inserts and spar cap.

IV. CONCLUSIONS

In this study, a glass-fibre reinforced composite blade demonstrator, which represents the main structure of a tidal turbine blade, was manufactured. Experimental structural testing was conducted to verify the performance of the demonstrator. The testing programme was performed in line with the IEC standard and includes a series of natural frequency tests and static tests. Instruments, including strain gauges, accelerometers, and displacement transducers, were installed on the demonstrator and steel fixtures to monitor the structure's responses. The demonstrator was found to fail under a load of 30.1 kN, where the steel inserts were pulled out. A comprehensive numerical model was developed to predict the structural responses of the demonstrator and steel fixtures. The accuracy of the proposed finite element model was validate against the testing data. Good agreements were found between the numerical prediction and the experimental results.

The study carried out in this research, relating to manufacturing, testing and numerical analysis of the demonstrator, will benefit the tidal turbine developers.

The experimental and numerical analysis results will help designers have an in-depth understanding on the performance of different rotor blade components. Moreover, it will benefit the composite structure manufacturers, as it verifies the reliability and strength of their products. This demonstrates the turbine blade's ability to withstand high tidal loadings, resulting in a reduction in maintenance costs and allowing for uninterrupted energy generation. This, in turn, will de-risk the technology and contribute to lowering the levelised cost of tidal energy.

REFERENCES

[1] OEE, Ocean Energy - Key trends and statistics 2021, Ocean Energy Europe, Brussels, Belgium, 2022. [Online]. Available: https://tethys-engineering.pnnl.gov/sites/default/files/publications/OEE-Stats-Trends-2021.pdf.

[2] T. R. Munaweera Thanthirige, J. Goggins, M. Flanagan, and W. Finnegan, "A State-of-the-Art Review of Structural Testing of Tidal Turbine Blades," *Energies*, vol. 16, no. 10, pp. 4061, 2023. DOI: 10.3390/en16104061, [Online].

[3] C. Glennon, W. Finnegan, N. Kaufmann, P. Meier, Y. Jiang, R. Starzmann, and J. Goggins, "Tidal stream to mainstream: mechanical testing of composite tidal stream blades to de-risk operational design life," *Journal of Ocean Engineering and Marine Energy*, vol. 8, pp. 163–182, 2022. DOI: 10.1007/s40722-022-00223-4, [Online].

[4] W. Finnegan, Y. Jiang, P. Meier, L.C. Hung, E. Fagan, and J. Goggins, "Numerical modelling, manufacture and structural testing of a full-scale 1 MW tidal turbine blade," *Ocean Engineering*, vol. 266, Issue 1, pp. 112717, 2022. DOI: 10.1016/j.oceaneng.2022.112717, [Online].

[5] E. Fagan, C.R. Kennedy, S.B. Leen, and J. Goggins, "Damage mechanics based design methodology for tidal current turbine composite blades," *Renewable Energy*, vol. 97, pp. 358-372, 2016. DOI: 10.1016/j.renene.2016.05.093, [Online].

[6] Y. Jiang, W. Finnegan, F. Wallace, M. Flanagan, T. Flanagan, and J. Goggins, "Structural analysis of a fibre-reinforced composite blade for a 1 MW tidal turbine rotor under degradation of seawater," *Journal of Ocean Engineering and Marine Energy*, 2023. DOI: 10.1007/s40722-023-00279-w, [Online].

[7] International Electrotechnical Commission - Wind turbine generator systems—part 23: full-scale structural testing of rotor blades, IEC 61400–23:2014.

[8] Ansys® Academic Research Mechanical, Release 2022R2 Help System. (2022). Mechanical Application Documentation, ANSYS, Inc.